Ms. Ref. No.: CATCOM-D-11-00457

11-Molybdo-1-vanadophosphoricacid $H_4PMo_{11}VO_{40}$ supported on ammonia-modified silica as highly active and selective catalyst for oxidation of methacrolein

Mitsuru Kanno[a], Yu-ki Miura[a], Toshiya Yasukawa[b], Toshio Hasegawa[b], Wataru Ninomiya[b], Ken Ooyachi[b], Hiroyuki Imai[c], Takashi Tatsumi[c], Yuichi Kamiya[d,]*

[a]Graduate School of Environmental Science, Hokkaido University, Kita 10 Nishi 5, Sapporo 060-0810, Japan

[b]Corporate Research Laboratories, Mitsubishi Rayon Co., Ltd., 20-1, Miyuki-cho, Otake, Hiroshima 739-0693, Japan

[c]Chemical Research Laboratory, Tokyo Institute of Technology, Nagatsuta 4259, Midori-ku, Yokohama 226-8503, Japan

[d]Research Faculty of Environmental Earth Science, Hokkaido University, Kita 10 Nishi 5, Sapporo 060-0810, Japan

*Corresponding author. Tel.: +81-11-706-2217; Fax: +81-11-706-2217; *E-mail adress*: kamiya@ees.hokudai.ac.jp;

ABSTRACT

Gas-phase oxidation of methacrolein to methacrylic acid has been carried out over various unsupported and supported $H_4PMo_{11}VO_{40}$ catalysts. While SiO_2-supported $H_4PMo_{11}VO_{40}$ showed low selectivity to methacrylic acid, $H_4PMo_{11}VO_{40}$ supported on NH_3-modified SiO_2, which was prepared by using an impregnation method with acetone as the solvent, exhibited high selectivity (~90%) and high activity for the formation of methacrylic acid. The activity of $H_4PMo_{11}VO_{40}/NH_3$-modified SiO_2 was more than five times higher than that of the corresponding unsupported catalysts.

Keywords:

Supported heteropolyacid; Ammonia-modified silica; Methacrylic acid; Selective oxidation

1. Introduction

Methacrylic acid (MAA), which is an important basic chemical, is prepared by gas-phase catalytic oxidation of methacrolein (MAL) (eq. 1).

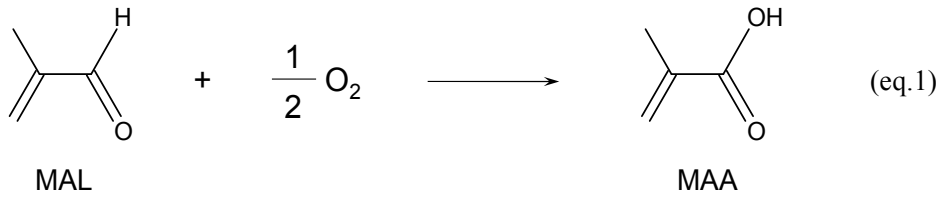

Heteropolyacids with a Keggin structure composed of P, Mo, and V have been utilized as industrial catalysts [1,2]. However, the catalytic performance, including activity and selectivity, must be improved.

Solid heteropolyacids, that is, unsupported heteropolyacids, often show low catalytic activities because of their low surface area. Supporting the heteropolyacids on oxide supports with high surface areas, especially SiO_2, increases the amount of the heteropolyacids exposed on the surface, leading to an enhancement in the catalytic activity [3]. In fact, several acid catalyzed reactions [4-14], as well as oxidation reactions [15-25] over supported heteropolyacid catalysts, have been reported so far. However, there are only a few reports on supported heteropolyacid catalysts being used for the gas-phase oxidation of MAL [26,27].

We have previously reported the gas-phase oxidation of MAL over SiO_2-supported $H_4PMo_{11}VO_{40}$ catalysts ($H_4PMo_{11}VO_{40}/SiO_2$) [28]. In fact, $H_4PMo_{11}VO_{40}/SiO_2$ shows much higher activity than unsupported $H_4PMo_{11}VO_{40}$ due to the high dispersion of $H_4PMo_{11}VO_{40}$ on SiO_2. However, $H_4PMo_{11}VO_{40}$ on SiO_2 undergoes thermal decomposition to form MoO_3 below a reaction temperature of 573 K. Since MoO_3 formed on SiO_2 accelerates the formation of CO_2 and acetic acid, $H_4PMo_{11}VO_{40}/SiO_2$ shows only low selectivity toward the formation of MAA [28].

Here we report that $H_4PMo_{11}VO_{40}$ supported on ammonia-modified SiO_2 (designated as NH_3-SiO_2) is a highly active and selective catalyst for the gas-phase oxidation of MAL to MAA. On NH_3-SiO_2, $H_4PMo_{11}VO_{40}$ did not decompose during the catalytic oxidation reaction due to the formation of a thermally stable crystalline NH_4^+ salt of $H_4PMo_{11}VO_{40}$. The stabilization and high dispersion of $H_4PMo_{11}VO_{40}$ led to not only high activity but also high selectivity for the formation of MAA in the gas-phase oxidation of MAL.

2. Experimental

2.1. Preparation of catalysts

$H_4PMo_{11}VO_{40}$ was prepared from MoO_3, V_2O_5, and 85% H_3PO_4 [28], which were

purchased from Wako Pure Chemical Co., Ltd. MoO_3 (31.7 g), V_2O_5 (1.82 g), and water (1.5 dm^3) were added to a round-bottom flask. After the addition of 85% H_3PO_4 (2.3 g) into the resulting suspension, it was heated and vigorously stirred at 358 K for 3 h. After the solution was cooled to room temperature, the insoluble matter was filtered off to obtain a clear orange solution. Then the solvent was evaporated to obtain $H_4PMo_{11}VO_{40}$ (designated as HPA), which was dried in air at 333 K overnight.

NH_3-SiO_2 was prepared according to a published method with some modifications [29]. SiO_2 (CARiACT Q-10 : 258 $m^2\ g^{-1}$, Fuji Silysia Chemical Ltd.) was treated in an N_2 flow at 1073 K for 1 h and then in an NH_3 flow (50 $cm^3\ min^{-1}$) at 1073 K for 4 h. The treated SiO_2 was then cooled to room temperature in an N_2 flow to obtain NH_3-SiO_2.

$H_4PMo_{11}VO_{40}$ supported on NH_3-SiO_2 was prepared by using an impregnation method with acetone as the impregnation solvent. After impregnation, the resulting wet solid was dried in air at 333 K overnight, followed by calcination in air at 523 K for 4 h. The obtained catalyst was designated as HPA[*acetone*]/NH_3-SiO_2. The loading amount of $H_4PMo_{11}VO_{40}$ was 43 wt%. For comparison, HPA[*water*]/NH_3-SiO_2 was prepared in a similar manner to HPA[*acetone*]/NH_3-SiO_2, except that water was used instead of acetone.

As a reference, one unsupported and two supported catalysts were prepared.

Unsupported $(NH_4)H_3PMo_{11}VO_{40}$ (designated as NH_4^+-HPA) was prepared by a titration method. An aqueous solution of NH_4NO_3 (0.1 mol dm^{-3}) was added to an aqueous solution of $H_4PMo_{11}VO_{40}$ (0.08 mol dm^{-3}), which was vigorously stirred, until the $NH_4^+/H_4PMo_{11}VO_{40}$ ratio reached unity. The resulting suspension was dried up, and then the resulting solid was dried in air at 333 K overnight.

$H_4PMo_{11}VO_{40}/SiO_2$ (designated as HPA/SiO_2) was prepared by impregnating SiO_2 with an acetone solution of $H_4PMo_{11}VO_{40}$ (0.08 mol dm^{-3}) in a similar manner to that for HPA[*acetone*]/NH_3-SiO_2. $(NH_4)H_3PMo_{11}VO_{40}/SiO_2$ (designated as [NH_4^+-HPA]/SiO_2) was prepared by adding an aqueous suspension of NH_4^+-HPA to SiO_2. The loading amount of $H_4PMo_{11}VO_{40}$ for all of the supported catalysts was 43 wt%.

All of the catalysts were calcined in air at 523 K for 4 h before use.

2.2. Characterization of catalysts

Powder X-ray diffraction (XRD) was performed using an X-ray diffractometer (Rigaku Mini Flex) with Cu Kα radiation (λ = 0.154 nm). Raman spectroscopy was performed using a laser Raman spectrometer (JASCO, RMP 200) with a 100-mW laser with a wavelength of 532 nm and a CCD detector. ^{31}P MAS-NMR spectra were recorded using a JEOL ECA-400

spectrometer with a spinning frequency of 7 kHz. All the measurements were carried out at room temperature. The chemical shifts are expressed relative to external 85% H_3PO_4.

2.3. Catalytic reaction

Catalytic oxidation of MAL was performed in a continuous flow reactor at 573 K and atmospheric pressure. Before the reaction, the catalyst was pretreated under a flow of a gas mixture consisting of O_2 (10.7 vol.%), H_2O (17.9 vol.%), and N_2 (balance) at a total flow rate of 28 cm^3 min^{-1} and a temperature of 593 K for 1 h. After the temperature was decreased to 573 K, a reactant gas mixture of MAL (3 vol.%), O_2 (6 vol.%), H_2O (15 vol.%), and N_2 (balance) was fed into the reactor to start the catalytic reaction. The amount of the catalyst and total flow rate were adjusted to control the conversion. The reaction products were analyzed by using on-line gas chromatographs (GCs) connected at the outlet of the reactor. For acetic acid (AcOH), MAL, and MAA, a GC (Shimadzu GC-14B) equipped with a flame ionization detector and a capillary column (TC-FFAP, 0.25 mm × 50 m) was utilized. For CO and CO_2, a GC (Shimadzu GC-8A) equipped with a thermal conductivity detector (TCD) and two packed columns (Molecular Sieve 5A, 2.85 mm × 3 m and Activated Carbon, 2.85 mm × 2 m) was used. In order to prevent interference from organic compounds, prior to the

GC–TCD analysis, the gas was passed through a dry-ice trap to remove them. As an internal standard for GC analysis, CH_4 (31%) diluted with He was mixed at the outlet of the reactor. The conversion of MAL was calculated by eq. 1.

$$\text{Conversion}(\%)=\frac{[\text{MAL}]_{\text{in}}-[\text{MAL}]_{\text{out}}}{[\text{MAL}]_{\text{in}}}\times 100 \qquad \text{eq. 1}$$

Here $[MAL]_{in}$ and $[MAL]_{out}$ are the concentrations of MAL at the inlet and outlet of the reactor, respectively.

3. Results and discussion

The catalytic data for the unsupported and supported catalysts for the gas-phase oxidation of MAL are summarized in Table 1. The activity and selectivity toward the formation of MAA of the unsupported HPA catalysts were 13 μmol g^{-1} min^{-1} and 75%, respectively (entry 1). Unsupported NH_4^+-HPA (entry 2), in which 25% of the H^+ of HPA was substituted with NH_4^+, was more selective for the formation of MAA (91% selectivity). However, the catalytic activity was similar to that of the unsupported HPA, indicating that the substitution of H^+ with NH_4^+ did not affect the activity. On the other hand, further

substitution of H^+ with NH_4^+ dramatically lowered the activity and selectivity for MAA (Fig. A1 in Supplementary data).

In the case of the supported catalysts (entries 3–6), the activities were more than 5 times higher than those for the unsupported HPA catalyst. However, the selectivity varied significantly depending on the support (SiO_2 or NH_3-SiO_2), impregnation solvent (acetone or water), and preparation method. HPA/SiO_2 exhibited the highest activity, although the selectivity for MAA was low (entry 3). The unsupported NH_4^+-HPA showed high selectivity to MAA (entry 2), whereas it was low for supported NH_4^+-HPA on SiO_2 (entry 4). On the other hand, HPA[*acetone*]/NH_3-SiO_2 showed the highest selectivity for MAA among the supported catalysts examined (entry 5). The catalyst was highly selective for MAA with a high conversion in comparison with that of [NH_4^+-HPA]/SiO_2 (Fig. 1). In addition, the catalytic performance of HPA[*acetone*]/NH_3-SiO_2 barely changed over at least 4 h (Fig. 2). However, HPA[*water*]/NH_3-SiO_2, which was prepared using water as the impregnation solvent, showed only low selectivity for MAA (entry 6). These results demonstrate that HPA[*acetone*]/NH_3-SiO_2 has potential for practical use.

It has been reported that substituting H^+ in unsupported $H_{3+x}PMo_{12-x}V_xO_{40}$ with Cs^+ ions is effective for suppressing the formation of byproducts, including acetic acid and CO_x, in the

gas-phase oxidation of MAL [30]. In fact, unsupported NH_4^+-HPA showed the highest selectivity for MAA (entry 2) among the catalysts examined, probably because of the lower number the acid sites due to the substitution of H^+ with NH_4^+ similar to unsupported $H_{3+x-y}Cs_yPMo_{12-x}V_xO_{40}$. However, [$NH_4^+$-HPA]/$SiO_2$ exhibited only limited selectivity for MAA (entry 4). In contrast, HPA[*acetone*]/NH_3-SiO_2 showed both high activity and high selectivity for MAA. To understand the differences in the selectivities among the supported catalysts, their structures were investigated before and after the reaction.

HPA[*acetone*]/NH_3-SiO_2 showed an XRD pattern identical to a crystalline NH_4^+ salt of $H_4PMo_{11}VO_{40}$ (cubic $(NH_4)_xH_{4-x}PMo_{11}VO_{40}$) [31] (Fig. A2(a) in Supplementary data), although the catalyst was prepared by supporting $H_4PMo_{11}VO_{40}$ on NH_3-SiO_2. The crystallite size of the NH_4^+ salt estimated from Scherrer's equation was 39 nm. In the ^{31}P MAS-NMR spectrum (Fig. A3(a) in Supplementary data), HPA[*acetone*]/NH_3-SiO_2 gave a intense peak at –4.4 ppm and relatively weak one at –3.6 ppm, which were assignable to the NH_4^+ salt of $H_4PMo_{11}VO_{40}$ and $H_4PMo_{11}VO_{40}$, respectively. The ^{31}P MAS-NMR spectrum indicated that the main species of the heteropolyacid formed on HPA[*acetone*]/NH_3-SiO_2 was $(NH_4)_xH_{4-x}PMo_{11}VO_{40}$. On the other hand, HPA/SiO_2 before the reaction showed an XRD pattern due to $H_4PMo_{11}VO_{40}\cdot 14H_2O$ microcrystallites (Fig. A2(b)) [32]. For

[NH_4^+-HPA]/SiO_2, strong and sharp diffraction lines attributed to cubic $(NH_4)_xH_{4-x}PMo_{11}VO_{40}$ and broad and weak ones due to $H_4PMo_{11}VO_{40}\cdot 14H_2O$ microcrystallites were observed (Fig. A2(c)), suggesting that relatively large-size $(NH_4)_xH_{4-x}PMo_{11}VO_{40}$ crystallites and dispersed $H_4PMo_{11}VO_{40}$ microcrystallites were present. In fact, the peak at –3.6 ppm due to $H_4PMo_{11}VO_{40}$ was strong comparing with the peak at –4.4 ppm due to $(NH_4)_xH_{4-x}PMo_{11}VO_{40}$ in the ^{31}P MAS-NMR spectrum for [NH_4^+-HPA]/SiO_2 (Fig. A3(c)). In a separate experiment (Supplementary data), the aqueous suspension of NH_4^+-HPA used for the preparation of [NH_4^+-HPA]/SiO_2 was separated using a centrifuge, affording a yellow solid and a clear orange solution. Elemental analysis and powder XRD indicated that the yellow solid was $(NH_4)_2H_2PMo_{11}VO_{40}$ crystallites and that the orange solution was an aqueous solution of the acid-form $H_4PMo_{11}VO_{40}$. Since [NH_4^+-HPA]/SiO_2 was prepared by adding such a suspension to SiO_2, large-size $(NH_4)_xH_{4-x}PMo_{11}VO_{40}$ crystallites and dispersed $H_4PMo_{11}VO_{40}$ microcrystallites coexist on the support. The structure of the heteropolyacid compounds in HPA[*water*]/NH_3-SiO_2 before the reaction was similar to that in [NH_4^+-HPA]/SiO_2 as evidenced by XRD pattern (Fig. A2(d)), and ^{31}P MAS-NMR spectrum (Fig. A3(d)).

After gas-phase oxidation of MAL, the structures of the supported catalysts were different. For HPA/SiO_2, the XRD lines due to $H_4PMo_{11}VO_{40}\cdot 14H_2O$ microcrystallites were

significantly less intense (Fig. 3b), and the Raman spectrum indicated the formation of molybdenum oxides (Fig. 4b) because the bands for molybdenum oxide phases (α-MoO_3 and β-MoO_3) were observed at 849, 820, 772, and 660 cm^{-1}, resulting in the low selectivity for MAA [28]. In the case of [NH_4^+-HPA]/SiO_2, the XRD pattern of $H_4PMo_{11}VO_{40}\cdot 14H_2O$ microcrystallites disappeared after the reaction (Fig. 3c), although it was clearly observed before the reaction. In addition, Raman bands attributed to MoO_3 were observed in the spectrum for NH_4^+-HPA/SiO_2 after the reaction (Fig. 4c). For HPA[*water*]/NH_3-SiO_2 after the reaction, Raman bands due to α-MoO_3 were present at 820 cm^{-1}. Thus, it is thought that some of the $H_4PMo_{11}VO_{40}$ microcrystallites on SiO_2 decompose to MoO_3 during the reaction in the cases of [NH_4^+-HPA]/SiO_2 and HPA[*water*]/NH_3-SiO_2. In contrast to these, HPA[*acetone*]/NH_3-SiO_2 showed only the XRD pattern (Fig. 3a) due to the cubic $(NH_4)_xH_{4-x}PMo_{11}VO_{40}$ even after the gas-phase oxidation of MAL. In addition, there were no Raman bands for MoO_3 after the reaction in the case of HPA[*acetone*]/NH_3-SiO_2 (Fig. 4a). Since there were a less amount of $H_4PMo_{11}VO_{40}$ crystallites in HPA[*acetone*]/NH_3-SiO_2, i.e., cubic $(NH_4)_xH_{4-x}PMo_{11}VO_{40}$ crystallites were mainly present, before the reaction, the heteropolyacid was hard to decompose to MoO_3 during the reaction. Thus, we concluded that the high dispersion of $H_4PMo_{11}VO_{40}$ on the support and the formation of the crystalline

NH_4^+ salt resulted in the high catalytic performance of HPA[*acetone*]/NH_3-SiO_2 for the gas-phase oxidation of MAL.

4. Conclusion

$H_4PMo_{11}VO_{40}$ supported on ammonia-modified SiO_2, which was prepared by using an impregnation method with acetone as the impregnation solvent, exhibited high selectivity (~90%) for the formation of methacrylic acid in the gas-phase oxidation of methacrolein. On the ammonia-modified SiO_2, $H_4PMo_{11}VO_{40}$ did not decompose to molybdenum oxide phases during the catalytic reaction due to the formation of thermally stable crystalline NH_4^+ salt of $H_4PMo_{11}VO_{40}$. The high dispersion of $H_4PMo_{11}VO_{40}$ on the support and the formation of the crystalline NH_4^+ salt lead to the high catalytic performance of the catalyst.

Appendix A. Supplementary data

Supplementary data to this article can be found online at doi:*xxxxxxxxxxxxxxxxxxx*.

References

[1] M. Wada, Petrotech 15 (1992) 452–458.

[2] M. Misono, N. Nojiri, Appl. Catal. 64 (1990) 1–30.

[3] T. Okuhara, N. Mizuno, M. Misono, Adv. Catal. 41 (1996) 113–252.

[4] J. Kaur, K. Griffin, B. Harrison, I.V. Kozhevnikov, J. Catal. 208 (2002) 448–455.

[5] J.X. Mao, Y. Kamiya, T. Okuhara, Appl. Catal. A 255 (2003) 337–344.

[6] L.A.M. Cardoso, W. Alves, A.R.E. Gonzaga, L.M.G. Aguiar, H.M.C. Andrade, J. Mol. Catal. A 209 (2004) 189–197.

[7] B.C. Gagea, Y. Lorgouilloux, Y. Altintas, P.A. Jacobs, J.A. Martens, J. Catal. 265 (2009) 99–108.

[8] K.A.D. Rocha, P.A. Robles-Dutenhefner, I.V. Kozhevnikov, E.V. Gusevskaya, Appl. Catal. A 252 (2009) 188–192.

[9] Y.D. Xu, Y.X. Qi, G.X. Lu, S.B. Li, Catal. Lett. 125 (2008) 83–89.

[10] A. Miyaji, R. Ohnishi, T. Okuhara, Appl. Catal. A 262 (2004) 143–148.

[11] H. Liu, N.H. Xue, L.M. Peng, X.F. Guo, W.P. Ding, Y. Chen, Catal. Commun. 10 (2009) 1734–1737.

[12] J.C. Juan, J.C. Zhang, M.A. Yarmo, J. Mol. Catal. A 267 (2007) 265–271.

[13] M.M.M.A. El-Wahab, A.A. Said, J. Mol. Catal. A 240 (2005) 109–118.

[14] K.A. da Silva, I.V. Kozhevnikov, E.V. Gusevskaya, J. Mol. Catal. A 192 (2003)

129–134.

[15] H. Liu, E. Iglesia, J. Phys. Chem. B 107 (2003) 10840–10847.

[16] L.M. Gomez Sainero, S. Damyanova, J.L.G. Fierro, Appl. Catal. A 208 (2001) 63–75.

[17] H. Kim, J.C. Jung, P. Kim, S.H. Yeom, K.-Y. Lee, I.K. Song, J. Mol. Catal. A 259 (2006) 150–155.

[18] Y. Liu, K. Murata, M. Inaba, N. Mimura, Catal. Commun. 4 (2003) 281–285.

[19] M. Sopa, A. Wącław-Held, M. Grossy, J. Pijanka, K. Nowińska, Appl. Catal. A 285 (2005) 119–125.

[20] N. Lingaiah, K.M. Reddy, P. Nagaraju, P.S. Prasad, I.E. Wachs, J. Phys. Chem. C 112 (2008) 8294–8300.

[21] R.D. Gall, C.L. Hill, J.E. Walker, Chem. Mater. 8 (1996) 2523–2527.

[22] Z. Karimi, A.R. Mahjoub, F.D. Aghdam, Inorg. Chim. Acta 363 (2009) 3725–3730.

[23] K.T. Venkateswara Rao, P.S.N. Rao, P. Nagaraju, P.S. Sai Prasad, N. Lingaiah, J. Mol. Catal. A 303 (2009) 84–89.

[24] P. Sharma, A. Patel, J. Mol. Catal. A 299 (2009) 37–43.

[25] Y. Kamiya, T. Okuhara, A. Miyaji, K. Tsuji, T. Nakajo, Catal. Surv. Asia 12 (2008)

101–113.

[26] H. Kim, J.C. Jung, D.R. Park, S.-H. Baeck, I.K. Song, Appl. Catal. A 320 (2007) 159–165.

[27] H. Kim, J.C. Jung, S.H. Yeom, K.-Y. Lee, I.K. Song, J. Mol. Catal. A 248 (2006) 21–25.

[28] M. Kanno, T. Yasukawa, W. Ninomiya, K. Ooyachi, Y. Kamiya, J. Catal. 273 (2010) 1–8.

[29] Y. Inaki, Y. Kajita, H. Yoshida, K. Ito, T. Hattori, Chem. Commun. (2001) 2358–2359.

[30] L.M. Deusser, J.C. Petzoldt, J.W. Gaube, H. Hibst, Ind. Eng. Chem. Res. 37 (1998) 3230–3236.

[31] N. Laronze, C. Marchal-Roch, N. Guillou, F.X. Liu, G. Hervé, J. Catal. 220 (2003) 172–181.

[32] T. Ilkenhans, B. Herzog, T. Braun, R. Schlögel, J. Catal. 153 (1995) 275–292.

Table 1

Catalytic data for gas-phase oxidation of methacrolein (MAL) over unsupported and supported $H_4PMo_{11}VO_{40}$ catalysts.

Entry	Type	Catalyst	Activity	Selectiviy[a]/%				(Conv.[b])
			/μmol g^{-1} min^{-1}	MAA	AcOH	CO_x	others	/%
1	Un-supported	HPA	13	75	5	16	4	8
2		NH_4^+-HPA	15	91	5	4	n.d.[c]	5
3	Supported	HPA/SiO_2	175	72	12	13	3	14
4		[NH_4^+-HPA]/SiO_2	71	65	14	17	4	6
5		HPA[*acetone*]/NH_3-SiO_2	76	89	4	7	n.d.[c]	9
6		HPA[*water*]/ NH_3-SiO_2	113	75	8	9	8	9

Reaction conditions: MAL:O_2:H_2O:N_2 = 3:6:15:76; temperature = 573 K, and total pressure = 0.1 MPa.

The activity and selectivity were estimated from the data obtained below 14% conversion.

[a]MAA: methacrylic acid, AcOH: acetic acid, and others: acetone, acetaldehyde, acrolein and acrylic acid.

[b]Conversions at which activity and selectivity were evaluated.

[c]Not detected.

Figure captions

Fig. 1. Relationship between selectivity and conversion for HPA[*acetone*]/NH_3-SiO_2 (closed symbols) and [NH_4^+-HPA]/SiO_2 (open symbols). (■,□) MAA, (◆,◇) acetic acid and (▲,△) COx. Reaction conditions: MAL:O_2:H_2O:N_2=3:6:15:76; temperature = 573 K, and total pressure = 0.1 MPa

Fig. 2. Time courses for the gas-phase oxidation of MAL over HPA[*acetone*]/NH_3-SiO_2. (●) Conversion of MAL and selectivities for (■) methacrylic acid, (◇) acetic acid, and (△) COx. Reaction conditions: MAL:O_2:H_2O:N_2 = 3:6:15:76, temperature = 573 K, total pressure = 0.1 MPa, and $W F^{-1}$ = 20 $g_{\text{-cat}}$ h $mol_{\text{-MAL}}^{-1}$

Fig. 3. XRD patterns for the supported $H_4PMo_{11}VO_{40}$ catalysts after gas-phase oxidation of MAL. (□) cubic $(NH_4)_xH_{4-x}PMo_{11}VO_{40}$ and (▲) $H_4PMo_{11}VO_{40}\cdot 14H_2O$. (a) HPA[*acetone*]/$NH_3$-$SiO_2$, (b) HPA/$SiO_2$, (c) [$NH_4^+$-HPA]/$SiO_2$, and (d) HPA[*water*]/$NH_3$-$SiO_2$. Reaction conditions: MAL:O_2:H_2O:N_2 = 3:6:15:76, temperature = 573 K, total pressure = 0.1 MPa, and 4 h.

Fig. 4. Raman spectra of the supported catalysts after the gas-phase oxidation of MAL. (●) MoO_3 phases (α-MoO_3 and β-MoO_3). (a) HPA[*acetone*]/NH_3-SiO_2, (b) HPA/SiO_2, (c) [NH_4^+-HPA]/SiO_2, and (d) HPA[*water*]/NH_3-SiO_2.

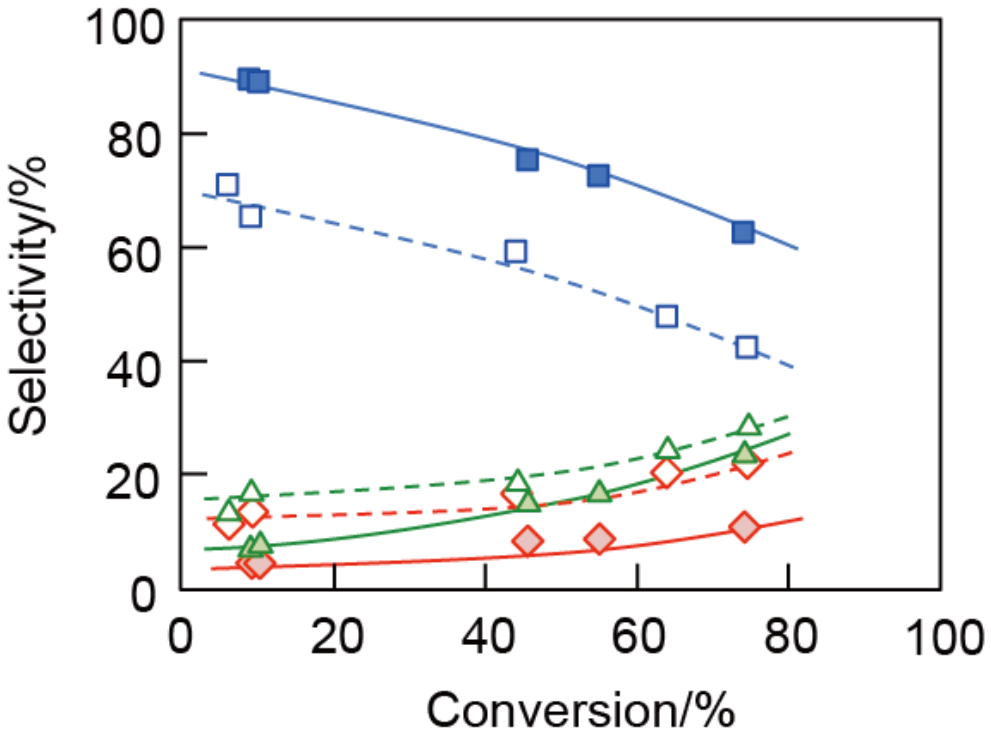

Fig. 1

Kanno et al.

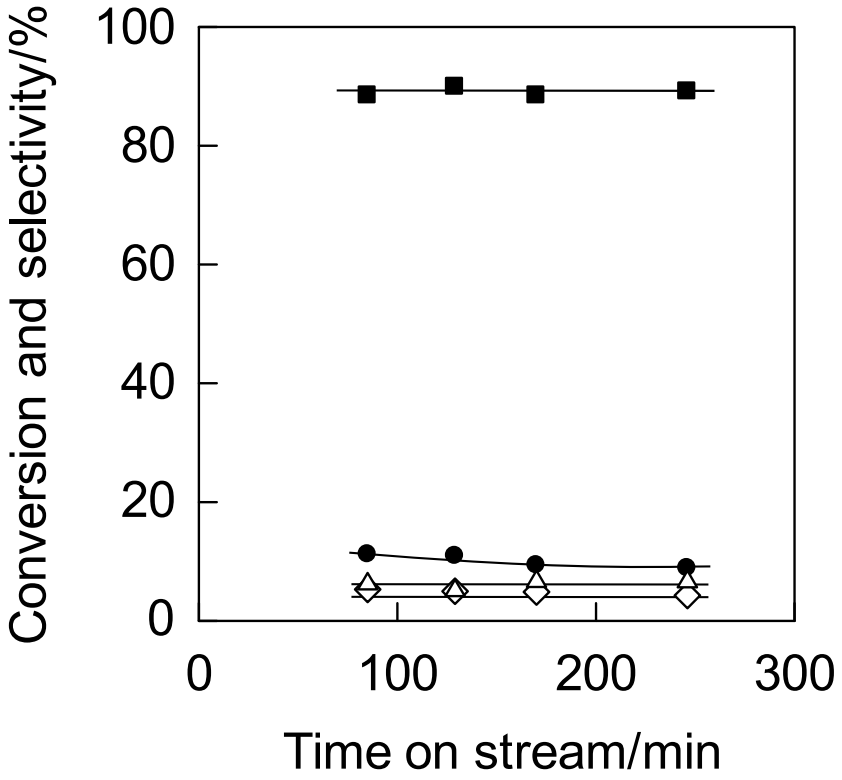

Fig. 2

Kanno et al.

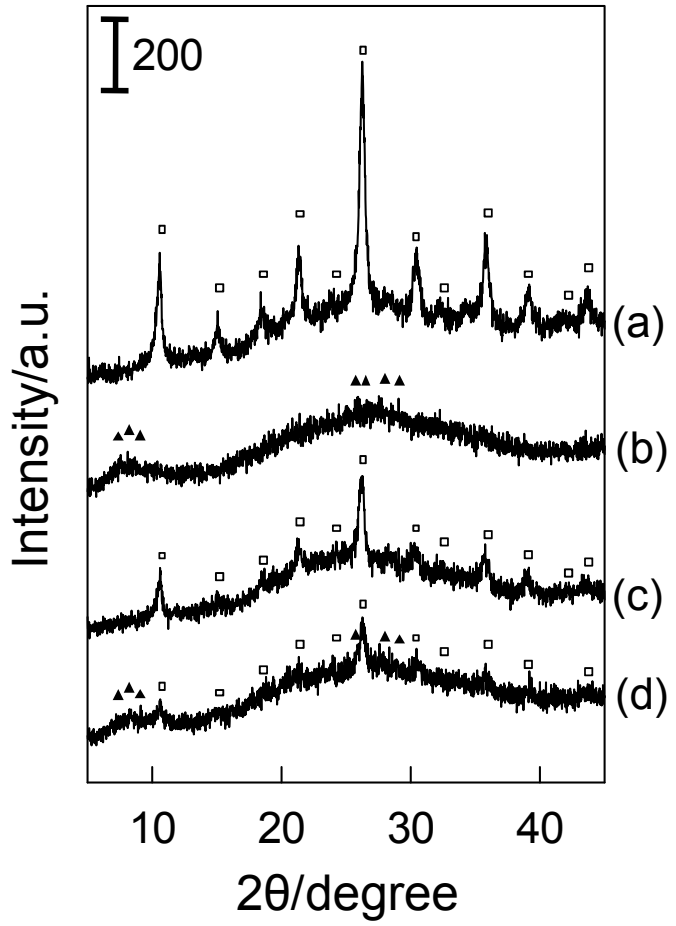

Fig. 3

Kanno et al.

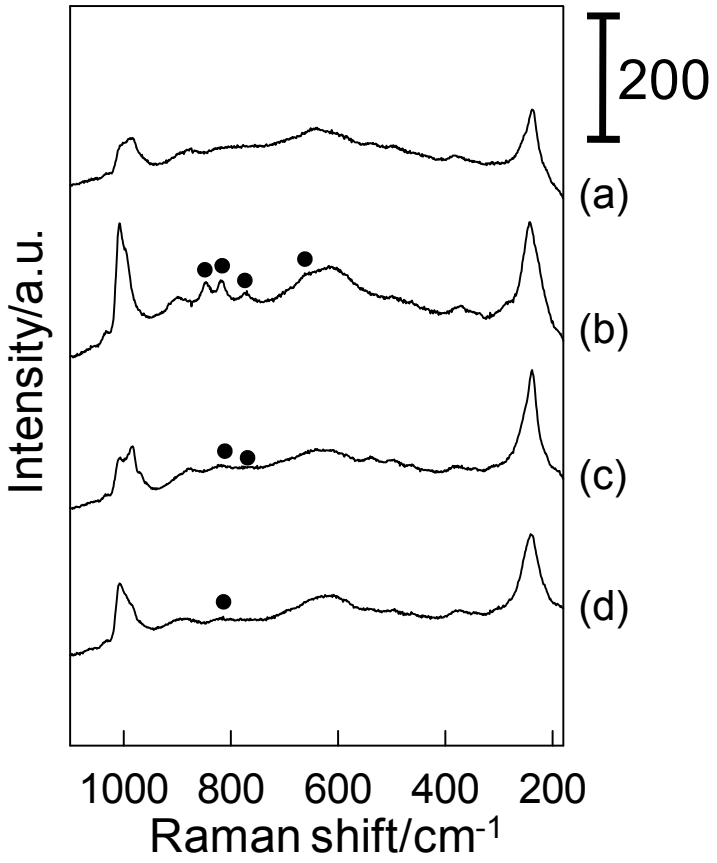

Fig. 4

Kanno et al.